HOT JUPITERS AND MAGNETIZED STARS: GIANT ANALOGS OF THE SATELLITE-JUPITER SYSTEM?

P. Zarka*

Abstract

Based on the observed correlation in our solar system between the output radio power of each planetary magnetosphere and the solar wind power incident on its magnetopause, and on the energetics of the interaction between Jovian Galilean moons and Jupiter's magnetic field (through Alfvén waves or magnetic reconnection), we derive a "generalized Radio-Magnetic Bode's law" relating the output radio power of a magnetized flow-obstacle system to the magnetic energy flux convected on the obstacle, this obstacle being magnetized or unmagnetized. A similar scaling law is found to also apply to satellite-induced UV emissions within the Jovian system. Extrapolation of this Radio-Magnetic Bode's law to the case of hot Jupiters suggests that these exoplanets may produce very intense radio emissions due to either magnetospheric interaction with a strong stellar wind or to unipolar interaction between the planet and a magnetic star (or strongly magnetized regions of the stellar surface). In the former case, similar to the magnetosphere-solar wind interactions in our solar system or to the Ganymede-Jupiter interaction, a hecto-decameter emission is expected in the vicinity of the planet with an intensity 10^3 to 10^5 times that of Jupiter's low frequency radio emissions. In the latter case, which is a giant analogous of the Io-Jupiter system, emission in the decameter-to-meter wavelength range near the footprints of the star's magnetic field lines interacting with the planet may reach 10^6 times that of Jupiter (unless some "saturation" mechanism occurs). The system of HD179949, where a hot spot has been tentatively detected near the sub-planetary point, is discussed in some details at the light of our above predicted energetics.

1 Introduction

In 1984 was introduced the so-called "radiometric Bode's law" [Desch and Kaiser, 1984] relating the auroral radio power emitted by Jupiter, Saturn and the Earth to the incident kinetic flow power on the magnetosphere's cross section

$$P_{flow} \sim NmV^3 \pi R_{\rm MP}^2 \tag{1}$$

* *Observatoire de Paris, LESIA, UMR CNRS 8109, 92195 Meudon, France*

with $N = N_o/d^2$ the solar wind (SW) number density (N_o being the density at Earth orbit and d the distance to the Sun in AU), V its velocity, $m \sim 1.1 \times m_p$, and $R_{\rm MP}$ the magnetopause radius. Zarka [1992, 1998] extended this law to the auroral radio emissions from Uranus and Neptune. In order not to mix auroral emissions resulting from the SW–magnetosphere interaction with similar emissions resulting from internal magnetospheric processes (as the Io-Jupiter interaction), Desch and Kaiser [1984] restricted the Jovian radio emission to the hectometer range ($\sim$ 200 kHz to 3 MHz). Zarka [1992, 1998] included the decameter emission independent of Io. The result, shown in Figure 1, is a striking correlation between the output planetary radio power and the SW power incident on the magnetopause (upper scale of x-axis), valid over about 4 orders of magnitude, with fluctuations below a factor of 2 of individual points around the best fit line. Moreover, the slope of this line is very close to 1, i.e. the output radio power is directly proportional to the input SW power. The proportionality constant is 10^{-5} (with $N_o = 5$ cm^{-3}).

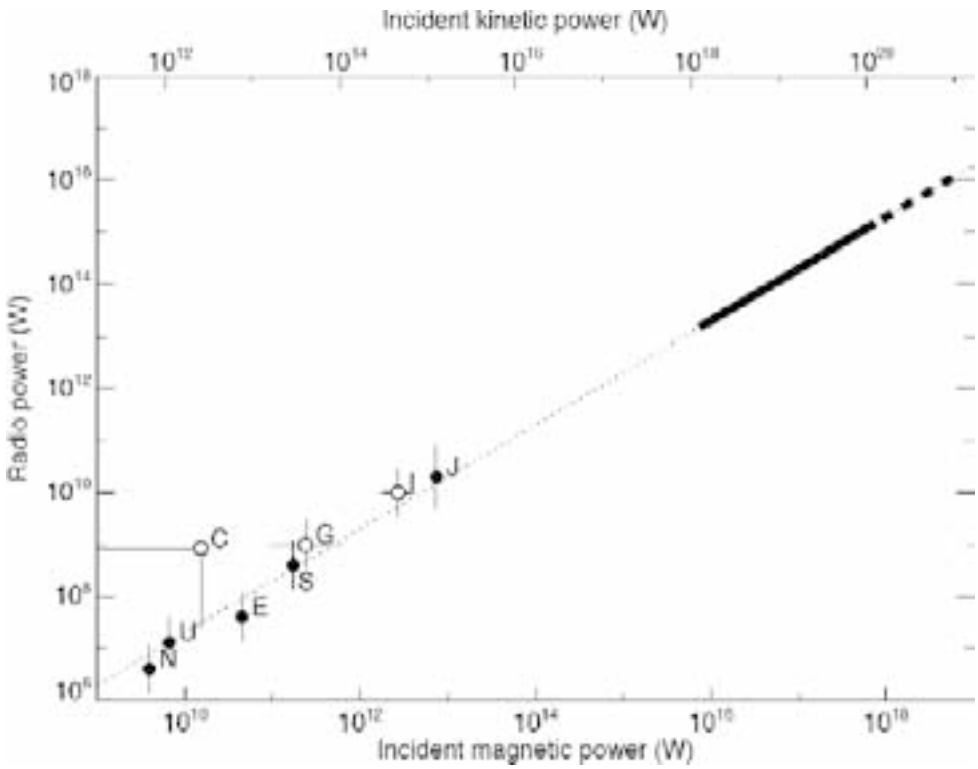

Figure 1: Generalized "Radio Bode's laws" showing the proportionality (slope $\sim$ 1) between output planetary radio powers and the SW power (kinetic or magnetic) incident on the magnetopause. E, J, S, U, N are the initials of the five radio planets. Kinetic-to-radio efficiency is $\sim 10^{-5}$, magnetic-to-radio efficiency is $\sim 2 \times 10^{-3}$. Open dots show the correlation between induced radio emissions from Io, Ganymede and an upper limit for Callisto, and dissipated magnetic power deduced from eq. (8) and Table 1. The thick bar results from extrapolation to hot Jupiters of the SW-planet interaction (solid) and unipolar star-planet interaction (dashed). [adapted from Zarka et al., 2001].

Noting that beyond $\sim$ 1 AU the SW magnetic energy density ($B^2/2\mu_o$, with B the interplanetary magnetic field – IMF) varies as the flow kinetic energy density ($\sim N m_p V^2$), i.e.

in $1/d^2$, the same correlation as above exists between the planetary auroral radio power and the IMF Poynting flux onto the magnetospheric cross-section

$$P_{IMF} = \int_{\mathrm{MP}} (\mathbf{E} \times \mathbf{B}/\mu_o) d\mathbf{S} \tag{2}$$

As $\mathbf{E} = -\mathbf{V} \times \mathbf{B}$, one finds that the radial component of $\mathbf{E} \times \mathbf{B}$ is equal to $VB_\perp^2$, thus

$$P_{IMF} = \frac{VB_\perp^2}{\mu_o} \pi R_{\mathrm{MP}}^2 \tag{3}$$

with $B_\perp$ the IMF component perpendicular to the SW flow in the planet's frame. The $1/d^2$ variation of the magnetic energy density results from the fact that the Parker spiral is already at 45° from the Sun–Earth direction at Earth orbit, and becomes nearly azimuthal beyond the orbit of Jupiter, thus $B \sim B_\varphi \propto 1/d$. As the SW magnetic energy density is ~ 170 times smaller that its flow kinetic energy density, the proportionality constant for the "Radio-Magnetic Bode's law" is $\sim 2 \times 10^{-3}$ (Figure 1, lower scale of x-axis). Although Saturn's kilometric radiation or Jupiter's hectometric radiation seem to correlate best on the short term with the SW pressure or kinetic energy flux [see e.g. Desch and Rucker, 1983; Zarka and Genova, 1983; Barrow and Desch, 1989], the IMF appears to be a decisive ingredient of the SW–magnetosphere coupling.

Zarka et al. [1997, 2001a] and Farrell et al. [1999, 2004a] applied these scaling laws to subsets of the recently discovered exoplanets around solar-type stars other than the Sun, especially the so-called "hot Jupiters", giant planets very close ($d < 0.1$ AU) from their parent star so that the incident stellar wind (SW) power is greatly enhanced as compared to solar system planets. They concluded that the output radio power of such systems should be 10^3 to 10^5 times larger than Jupiter's one, and consequently near the lower limit of the radio flux densities detectable over sky background fluctuations with present large ground-based radiotelescopes in the decameter–to–meter wavelength range.

This is true only if these exoplanets have a maximum surface magnetic field of at least 5 to 10 G, and thus a magnetic moment $\geq 0.5 \times \mathcal{M}_J$ (with $\mathcal{M}_J$ the Jovian magnetic moment), so that electrons accelerated through the SW–planet interaction can precipitate along the planet's magnetic field lines towards its auroral regions and produce there intense radio emissions at decameter wavelengths. However, all empirical laws used for predicting magnetic field generation by the planetary dynamo involve a term P_{sid}^α where P_{sid} is the sidereal planetary rotation period and $-1 \leq \alpha \leq -1/2$ (see appendix of [Farrell et al., 1999] and [Griessmeier et al., 2004]), i.e. the predicted planetary field decreases with increasing sidereal rotation period. For hot Jupiters, strong tidal interactions are expected to lead (in $\leq 10^{6--7}$ years ? [M. Ollivier, personal communication; see also Burns, 1986]) to planetary spin-orbit synchronization, and thus to sidereal rotation slowing (down to 3 – 4 day periods) and decay of the magnetic moment. Recent estimates by Sanchez-Lavega [2004] based on internal structure and convection studies give upper limits of 1.5 to 6 G for the surface field of hot Jupiters (versus 8 to 14 G for Jupiter). One important question is thus: "How are the above scaling laws modified in the case of a weakly magnetized or unmagnetized exoplanet, and what can we predict in terms of radio emission output ?". To answer this question, we will rely upon the similarity of such systems with the Jupiter–satellite systems, well studied in recent past years using ground-based and spacecraft measurements.

In this paper, we study how the high latitude radio (and to a lesser extent the UV) emissions associated with satellite-magnetosphere interactions compare to the power dissipated in the interactions, and how the deduced efficiencies compare to the above scaling laws. In section 2, we describe the two types of satellite-Jupiter interactions and evaluate the corresponding dissipated powers. In section 3 we evaluate the energetics of the electromagnetic (UV and radio) emissions produced by these interactions, compare them to the dissipated powers, and derive a "generalized Radio-Magnetic Bode's law". In section 4 we apply this generalized scaling law to the case of hot Jupiters. In section 5 we briefly comment the first observations interpreted as a star–exoplanet "plasma" interaction (in the system of HD 179949). Section 6 summarizes our results and briefly discusses radio observations of candidate exoplanets.

2 Satellite – Jupiter interactions

Due to the strong magnetic field intensity and low plasma density in the Jovian magnetosphere, the magnetic energy ($B^2/2\mu_o$) convected onto/past a galilean satellite is much larger than the kinetic energy ($\sim NmV^2$) of the magnetospheric (corotating) plasma flow, a situation opposite to the SW–magnetosphere case: at Io's orbit, for example, the Jovian magnetic field is $B \sim 0.02$ G, the relative velocity between the corotating magnetospheric field and plasma Io's orbital motion is $V \sim 57$ km/s, and the maximum plasma number density reaches $N \sim 2000$ cm^{-3} in the Io torus, with a typical molecular mass $m \sim 20 \times m_p$. The corresponding ratio $(B^2/\mu_o)/(NmV^2)$ is about 15.

Two types of moon-magnetosphere interaction have been observed at Jupiter.

When the satellite is magnetized, as is the case for Ganymede, it develops its own magnetosphere, embedded in that of Jupiter. Interaction between the satellite and the Jovian magnetic field is believed to happen primarily through continuous reconnection of the satellite's and the planet's magnetic fields [Kivelson et al., 1997a] (Figure 2). Such an interaction may be qualified of "dipolar". Note that the radius of Ganymede's magnetopause is about 2.5 to 3 times the radius of the moon itself [Gurnett et al., 1996; Kivelson et al., 1996, 2004].

When the satellite is unmagnetized, as is the case for Io or Europa, its ionosphere (and induced field) interacts with the Jovian field through MHD waves (Alfvén waves, slow mode waves or slow mode shocks) generating "wings" across the jovian field downstream of the satellite [Neubauer, 1980; Erkaev et al., 2002; Kivelson et al., 2004; Saur et al., 2004] (Figure 3). Such an interaction may be qualified of "unipolar", although strictly speaking the "unipolar inductor" case corresponds to very large Alfvén velocities between the satellite and the planet and thus quasi-instantaneous setup of a field-aligned current circuit [Goldreich and Lynden-Bell, 1969]. When the satellite-planet Alfvén travel time is longer that the convection time of the magnetospheric field and plasma past the satellite, "wings" are generated as the envelope of the perturbation travelling from the satellite to the planet in both hemispheres. In that case, the high latitude signatures of the satellite-magnetosphere interaction (see section 3) are shifted from the instantaneous satellite longitude, leading it by an angle $\delta = 2\pi t_A/P_{syn}$ (with t_A the Alfvén travel time and P_{syn}

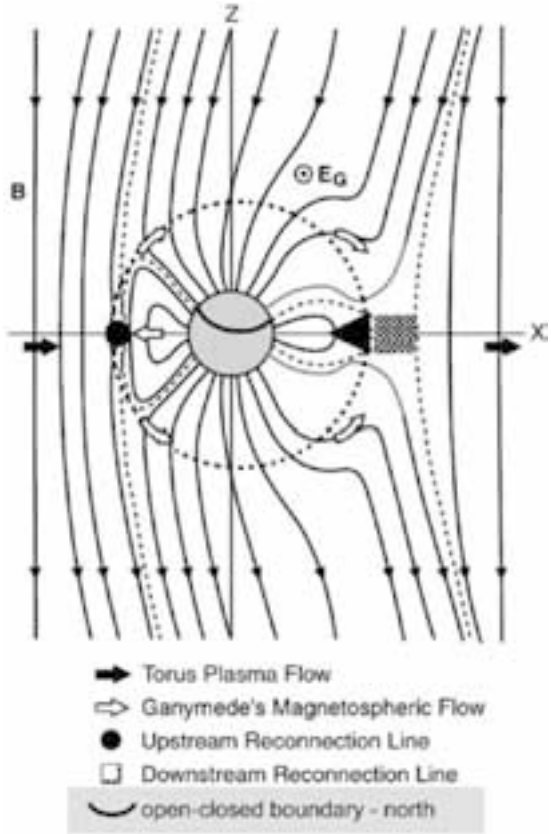

Figure 2: Fields and flows in the vicinity of Ganymede. Y axis points towards Jupiter. The extent of Ganymede's magnetosphere (i.e. Ganymede-dominated field region) is represented as the dotted sphere of radius $\sim 2.5\ R_G$. *[adapted from Kivelson et al., 2004].*

the planetary rotation period as seen from the satellite – see Fig. 6 of [Zarka, 2004]). $\delta = 3° - 20°$ in the Io-Jupiter case. This angle is modified by the planetary magnetic field topology because field lines are not necessarily contained in a meridian plane. From the Jovian O6 and VIP4 internal field models of Connerney [1992] and Connerney et al., [1998], the longitude of the instantaneous Io field line footprint may differ by $\pm 40°$ from that of Io, thus finally $\delta = -37°$ to $+60°$. For such an interaction between an unmagnetized satellite and the Jovian field, the radius of the obstacle to be considered is the typical exo-ionospheric radius, taken as $1.1\times$ to $1.4 \times R_{Io}$ in the case of Io [Kivelson et al., 1997b].

The power dissipated through the "dipolar" interaction (P_d) can be estimated from the reconnected magnetic flux at the magnetopause. Following Akasofu [1981, 1982] we can express the SW-magnetosphere reconnected power as the Poynting flux on the magnetopause cross-section, or equivalently (following eq. 2) :

$$P_d = \varepsilon \frac{KVB_\perp^2}{\mu_o} \pi R_{\mathrm{MP}}^2 \tag{4}$$

with ε a reconnection efficiency of the order of 0.1–0.2, and K a function that "triggers" the reconnection in response to the magnetosphere state (open or closed). Depending on

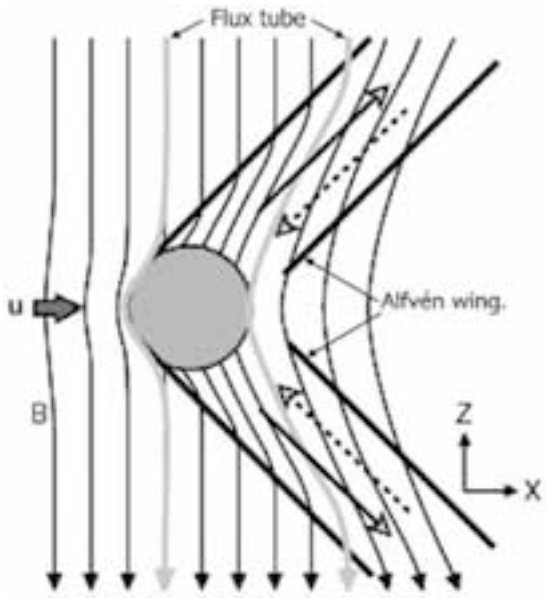

Figure 3: Sketch of Io's Alfvén wing across Jupiter's magnetic field (B, southward). **u** *represents the incident flow velocity. Y axis points towards Jupiter. Solid (resp. dashed) arrows – with open heads – represent currents flowing on the anti-Jupiter (resp. on the Jupiter) side of the IFT. [adapted from Kivelson et al., 2004].*

the orientation of the planetary dipole field, $K = \sin^4(\theta/2)$ (for Earth) or $\cos^4(\theta/2)$ (for Jupiter and Saturn), θ being the angle between the IMF and the planetary field. The relative orientation of Ganymede's field and of the Jovian field is such that $K \sim 1$ (open magnetosphere case). Thus, the dissipated (reconnected) power may be written :

$$P_d \sim \varepsilon \frac{V B_\perp^2}{\mu_o} \pi R^2_{\mathrm{MP-Ganymede}} \tag{5}$$

i.e. it is a fraction ε of the incident Poynting flux ($V B_\perp^2/\mu_o$) on the obstacle of cross-section (πR^2_{MP}, with $R_{\mathrm{MP}} \sim 2.5 - 3 \times R_G$). The strongly magnetized environment of Ganymede leads to expect a value of ε larger than in the Earth's magnetosphere case, up to 0.3 [Kivelson et al., 1997a].

In the case of the Io-Jupiter "unipolar" interaction, the dissipated power has been estimated via several mutually consistent approaches. The potential drop across the obstacle (Io's ionosphere) is

$$\phi = E \times 2R_{obs} = V \times B_\perp \times 2R_{obs} \tag{6}$$

with $V = 57$ km/s, $B_\perp = B_J$ the Jovian field at Io's orbit (~ 0.02 G), thus $E \sim 0.1$ V/m, and $R_{obs} = (1.1 - -1.4) \times R_{Io}$, thus $\phi \sim 500$ kV. The Voyager 1 spacecraft deduced from magnetic field perturbations measured near Io that a current of intensity $I = 2 - -3 \times 10^6$ Amperes was circulating in the Io flux tube (IFT), thus a first crude estimate of the dissipated power

$$P_d = I \times \phi \sim 10^{12} \text{ W} \quad \text{(per hemisphere)}$$

A nonlinear MHD analysis of the Io-Jupiter circuit led Neubauer [1980] to infer the existence of currents perpendicular to the Jovian magnetic field in the Alfvén wings, contributing to close the Io current circuit (instead of Jupiter's ionosphere only in the unipolar inductor case of Goldreich and Lynden-Bell [1969]). Neubauer [1980] expressed the Alfvén conductance

$$\Sigma_A = \frac{M_A}{\mu_o V \sqrt{1 + M_A^2}}$$

when the flow is strictly perpendicular to the field ($M_A = V/V_A$ is the Alfvén Mach number, with $V_A = B/\sqrt{Nm\mu_o}$, and derived a dissipated power

$$P_d = \Sigma_A \times E^2 \times \pi R_{obs}^2 \sim 10^{12} \text{ W} \quad \text{(per hemisphere)} \tag{7}$$

Following Zarka et al. [2001a], we rewrite the above expression (7) as

$$P_d = \frac{1}{\sqrt{1 + M_A^{-2}}} \frac{V B_\perp^2}{\mu_o} \pi R_{obs}^2$$

This expression is identical to (4) except for the factor $1/\sqrt{1 + M_A^{-2}}$ (instead of ε). Whatever the value of M_A, one has

$$M_A \leq \frac{1}{\sqrt{1 + M_A^{-2}}} \leq 1$$

The Io-Jupiter interaction occurring in sub-Alfvénic regime, with $M_A = 0.15$ to 0.3, implies $1/\sqrt{1 + M_A^{-2}} = 0.15$ to 0.3 also, thus very similar to the expected value for ε. The detailed values of the efficiency also depends (through E) on the conductivity of the obstacle.

We infer thus a general estimate for the power dissipated P_d via a satellite-magnetosphere interaction, be it "unipolar" or "dipolar":

$$P_d \sim \frac{\varepsilon V B_\perp^2}{\mu_o} \pi R_{obs}^2 \tag{8}$$

This very general expression is simply the fraction ε of the magnetic energy flux convected on the obstacle. It is expected to provide a correct order of magnitude whatever the interaction regime (super- or sub-Alfvénic), as long as the obstacle conductivity is not vanishingly small. At Io, the obstacle is the extended exo-ionosphere, of radius $(1.1 - -1.4) \times R_{Io}$. At Ganymede, the obstacle is the magnetopause, of radius $(2.5 - -3.0) \times R_G$. At Europa and Callisto, conductivity may be provided by a subsurface ocean [Khurana et al., 1998] and/or an extended plasma cloud of density up to $100 - -400$ cm^{-3} [Kurth et al., 2000; Gurnett et al., 2000]. We will use for these two satellites an obstacle size between 1.0 and 1.2 times their diameter.

Table 1 lists the predicted values of P_d for Jupiter's four galilean satellites, computed with $\varepsilon = 1$ (the efficiency will be included in the "Radio-Magnetic Bode's law" – see below). It is remarkable that P_d is similar for Europa and Ganymede, with a value

Table 1: For each galilean satellite we list: the orbital distance in R_J (1 R_J = 71400 km); the (min-max) Jovian field amplitude at the satellite orbit, computed from the O6 or VIP4 internal field model with current sheet; the relative velocity $V = V_{\rm corot} - V_{\rm orb} = \Omega_J L R_J - \sqrt{GM_J/LR_J}$; the estimated obstacle size as discussed in the text; the deduced upper/lower limit of the maximum dissipated power following eq. (8) with ε=1; the estimated emitted UV power, (+) reminding that Ganymede's UV emission are generally brighter than Europa's; the estimated radio power (see section 3); the qualitative interaction strength (from [Kurth et al., 2000]).

Satellite	Io	Europe	Ganymede	Callisto
L [R_J]	5.9	9.4	15	26.4
B_J [G]	$(1.8-2.1)\cdot 10^{-2}$	$(4.0-5.0)\cdot 10^{-3}$	$(0.7-1.5)\cdot 10^{-3}$	$(0.5-4.7)\cdot 10^{-4}$
V [km/s]	57	104	177	323
R_{obs} [km]	$(1.1-1.4)\cdot 1820$	$(1.0-1.2)\cdot 1560$	$(2.5-3.0)\cdot 2630$	$(1.0-1.2)\cdot 2410$
P_d [W/hem.]	$(1.8-4.1)\cdot 10^{12}$	$(1.0-2.3)\cdot 10^{11}$	$(0.9-6.2)\cdot 10^{11}$	$(0.1-15.)\cdot 10^{9}$
P_{UV} [W]	$(2-10)\cdot 10^{10}$	$(1-10)\cdot 10^{9}$	$(1-10)\cdot 10^{9}(+)$	?
P_{Radio} [W]	$0.3-3\cdot 10^{10}$	?	$\sim 10^{9}$	$\leq 8.5\cdot 10^{8}$
Interaction	Strongest	Intermediate	Intermediate	Weakest

$\sim$ 10 times smaller than in Io's case. Although Ganymede is farther from the planet, hence a magnetic energy density $\sim$ 20 times weaker at Ganymede's orbit than at Europa's, its magnetosphere has an electrodynamic cross-section $\sim$ 20 times as large as Europa's conductive interior/envelope. P_d is weaker for Callisto, but also much more variable due to the crossing by Callisto of the Jovian current disk twice per Jovian rotation. The maximum value of P_d for Callisto is only six times weaker than the minimum dissipated power for Ganymede and Europa.

3 Energetics of induced electromagnetic emissions

Whatever the interaction type, "unipolar" or "dipolar", it should lead to field-aligned currents circulating between the satellite and the planet. Due to the low magnetospheric electron density, the necessity to sustain these currents leads to electron acceleration [Knight, 1973]. Electrons precipitating towards high Jovian latitudes in/near the IFT have an energy of several keV to tens of keV [Prangé et al., 1996; Zarka et al., 1996]. They produce an induced aurora in the form of a bright UV spot in the atmosphere due to collisionnal excitation of atmospheric species (mainly H and H_2). The intensity of this spot varies with the longitude and corresponds to a radiated UV power of $2--10\times 10^{10}$ W (in H Ly-α and H_2 Lyman and Werner bands), requiring a $1--6\times 10^{11}$ W precipitation power under the form of 10–100 keV electrons [Prangé et al., 1996, 1998 ; Clarke et al., 2002]. The IFT's northern and southern footprints have also been detected in the IR (H_3^+) [Connerney et al., 1993] and require a similar precipitation power. On recent HST UV images of northern Jovian auroral regions, one can see clearly the bright footprints of Ganymede's and Europa's flux tubes (Figure 4). Only a few quantitative measurements have been published so far about these footprints. Clarke et al. [2002] estimated their brightness to be one order of magnitude weaker than the IFT footprint (10's of kilorayleighs for Ganymede and Europa, 100's of kilorayleighs for Io). They also note that Ganymede's

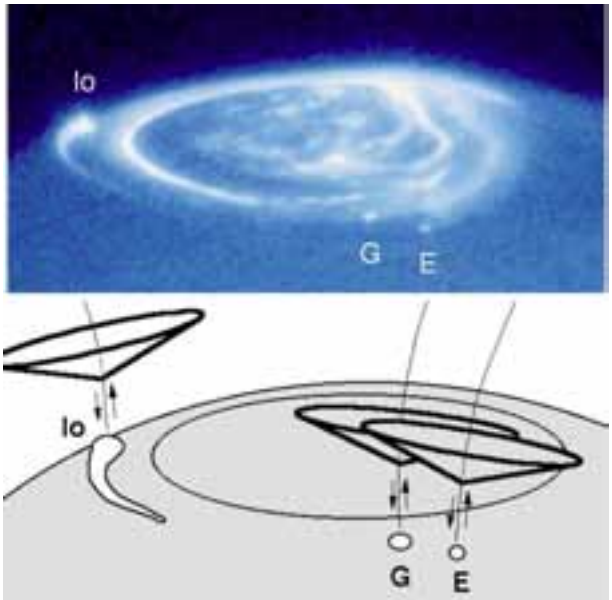

Figure 4: HST UV image of northern Jovian auroral regions, showing clearly the bright footprints of Io (plus a tail-like structure), Ganymede and Europa flux tubes. The sketch below represents radio emission hollow conical beams produced above the UV hot spots by the energetic electrons precipitated along the satellites flux tubes or reflected upwards by magnetic mirrorring. Courtesy R. Prangé , L. Pallier, and J.T. Clarke.

footprint is generally brighter than Europa's one. Taking into account the smaller spot sizes (as compared to Io's), one obtains a radiated UV power about $1 - -10 \times 10^9$ W for Ganymede and Europa [Clarke et al., 2002; Prangé and Zarka, 2003]. No UV spot has been detected at Callisto's flux tube footprint, but this is due to the fact that this footprint would lie directly inside the main auroral oval.

The energetic electrons precipitated along the satellites flux tubes or reflected upwards by magnetic mirrorring also produce intense nonthermal radio emissions (Figure 4). The radio output power is more difficult to estimate than the UV one because the absence of angular resolution of low-frequency radio measurements implies that the satellite-induced nature of part of the observed emissions is determined on a statistical basis. The best available estimate for the average detected power of Io-induced radio emissions, derived from integration over time, emission bandwidth and beaming pattern, is $\sim 10^{10}$ W [Kaiser et al., 2000; Queinnec and Zarka, 2001; Zarka et al., 2004]. Instantaneous values typically span the range $0.3 - -3 \times 10^{10}$ W, which requires $3 - -10 \times 10^{11}$ W precipitations in 1–10 keV electrons. Less accurate estimates are available for Europa, Ganymede, and Callisto. Menietti et al. [1998, 2001] have searched for the influence of these satellites on Jupiter's hecto-decameter emission by analyzing Galileo/PWS observations in the range $2.0 - -5.6$ MHz. The results have been synthesized and compared to Cassini/RPWS observations by Hospodarsky et al. [2001]. The occurrence and intensity of radio emissions detected by Galileo above a threshold of 4×10^{-18} W/m^{2}Hz were binned in $6° \times 6°$ longitude $\times$ satellite phase (with respect to the observer) and normalized to a fixed observer distance. Increased occurrence probability and average intensity were found at

specific orbital phases of Ganymede and Callisto. The average isotropic power in high intensity bins are $\sim 4 \times 10^7$ W for Ganymede and Callisto, versus 5.6×10^7 W for Io [Menietti et al., 2001]. But occurrence rates of induced emissions are much weaker for the former. The occurrence probability of Io-induced emission is typically ~ 1.6 times that of the satellite-independent one (as deduced by comparing peak amplitude to baseline level in Fig. 2 of Hospodarsky et al. [2001]). For Ganymede, the occurrence probability is $0.029/0.18 = 0.16$ that of the satellite-independent emissions, and $\leq 0.025/0.18 = 0.14$ for Callisto (the latter case being very noisy). Referring to a 10^{10} W average power for the Io-induced emission, and assuming similar bandwidth and beaming patterns for all satellite-induced emissions, one gets rough estimates of 10^9 W for Ganymede and an upper limit of 8.5×10^8 W for Callisto. No Europa-induced radio emission was found. This may be due to the 4:2:1 orbital resonance between Io, Europa and Ganymede, which may "hide" weak Europa-induced radio emissions in stronger Io- or Ganymede-induced ones. No correlation of radio emissions with satellites other than Io could be found in the limited Cassini/RPWS database.

Finally, based on local wave observations by Galileo, Kurth et al. [2000] have qualitatively classified the interaction strength of the 4 galilean satellites with Jupiter's magnetic field: not surprisingly, Io has the strongest interaction; Europa and Ganymede are "intermediate", and Callisto has the weakest interaction. This, and the fact that 8.5×10^8 W represents an exceedingly large fraction of the available power at Callisto's orbit, further suggests that the radio powers derived above for Callisto are truly upper limits.

Table 1 summarizes the estimates discussed above for the energetics of induced electromagnetic emissions, as well as the interaction strength "classification". With the exception of P_{Radio}(Callisto), comparison of the last 4 columns shows a consistent relationship between the radiated powers, interaction strength, and predicted dissipated powers. The overall UV efficiency (P_{UV}/P_d) is 1 – 5%, and the Radio efficiency ($P_{\rm Radio}/P_d$) is 0.2 – 1%. The latter range includes the "Radio-Magnetic Bode's law" from section 1 (0.2%), so that on Figure 1, the points representing the Io- and Ganymede-Jupiter interactions fall close to the best fit line. We obtain thus empirically a "generalized Radio-Magnetic Bode's law" relating the output radio power of a magnetized flow-obstacle system to the magnetic energy flux convected on the obstacle :

$$P_{\rm Radio} \sim \eta \times P_d \tag{9}$$

with $\eta \sim 2 - -10 \times 10^{-3}$. P_d is given by eq. (8) with $\varepsilon = 1$ and represents the upper limit of the dissipated power. The uncertainty on the fraction of this power actually dissipated (contained in the precise value of $\varepsilon < 1$) can be included in the efficiency parameter η.

Note that Akasofu [1982] already concluded that the total energy output (or "consumption") of the Earth's magnetosphere, as defined via geomagnetic indexes, correlated best with the reconnected magnetic power expressed by equation (8) (rather than with the SW kinetic energy flux). Note also that on the basis of equations (8–9), Zarka et al. [2001a] argued that Dione has a too small cross section with with Saturn's magnetic field to influence SKR in any significant way, as was nevertheless suggested by Voyager observations [Kurth et al., 1981; Desch and Kaiser, 1981]. Should Cassini, on the basis of long term measurements, demonstrate that the effect is truly there, then it would imply

a significantly larger cross section for Dione (of order 10×) due, perhaps, to a substantial intrinsic magnetic field or more probably an extended exosphere.

One may think from Table 1 that, similarly, a "UV-Magnetic Bode's law" could be defined. But this proves to be difficult because (i) the main auroral ovals at the various planets has different physical origins (SW coupling/reconnection at Earth, corotation breakdown at Jupiter, still discussed at Saturn...), and (ii) the radiated UV power depends not only on the precitated particles' nature and energy, but also on atmospheric composition (plus radiative transfer). Thus, a correlation valid for various emissions at one single planet (as in Table 1) may be difficult to generalized to all auroral UV emissions. By contrast, radio emissions are directly emitted by precipitated (mirrored) electrons of energy 1–10 keV, and in Figure 1 each radio components was related – as far as possible – to the corresponding flow-obstacle interaction driving it (e. g. only the hecto-decameter emission independent of Io was used for $P_{\mathrm{Radio}}(J)$). Finally, as we discuss below the remote detection of electromagnetic signatures of exoplanet-star plasma interactions, the low-frequency radio range has the great advantage of a star-planet contrast ~ 1 (Jupiter's decameter emissions are approximately as intense as Solar decameter radio bursts [Zarka et al., 1997; Zarka, 2004]), versus 10^{6--9} in the UV range.

4 The case for "hot Jupiters"

Out of 168 exoplanets known at the time of this writing (within 144 planetary systems – cf. [Schneider, 2005]), 27 (16%) have a semi-major axis ≤ 0.05 AU (or $\sim 10\ R_S$, with $R_S = 7 \times 10^8$ m the solar radius and 1 AU $\simeq 213.7\ R_S$), and 39 (23%) have a semi-major axis ≤ 0.1 AU. These are called "hot Jupiters" due to their strong irradiation. As noted by Zarka et al. [2001a], these planets, when orbiting a solar-type star, receive from the wind of their parent star an energy flux 10^3 to 10^5 times larger than at Jupiter's orbit. Stronger stellar winds, as those occurring in young stellar systems [see Griessmeier et al., 2005; Stevens, 2005; and references therein], would of course lead to still higher power inputs.

By analogy with the solar wind, the stellar wind plasma is expected to carry away frozen-in magnetic field from the star through the interplanetary medium. In the case of the Sun, the large scale dipolar field has a surface intensity about 1 to 1.5 G. Magnetic spots and associated loops may exhibit magnetic field intensities of 10^3 G [Priest, 1995]. Stellar surface magnetic fields of the order of 10^3 G are not uncommon (so-called magnetic stars) [see e. g. Saar, 1996].

As discussed in section 1, exoplanets may have a strong (Jovian-like) magnetic field, but they may also be weakly magnetized or unmagnetized due to tidal spin-orbit synchronization. The type of planet-star "plasma" interaction will of course strongly depend on the magnetic field of each of the two bodies involved.

4.1 Magnetospheric interaction

If the planet is strongly magnetized (surface field above a few Gauss), then it will have a developed magnetosphere interacting with the stellar wind and its magnetic field in a way similar to the Earth's or Jupiter's magnetosphere with the solar wind. This interaction probably involves reconnection at the magnetopause as discussed above. It may be considered "dipolar", and its maximum strength evaluated according to expression (8) (with $\varepsilon = 1$), as already suggested by Zarka et al. [2001a]. Making an analogy with RSCVn magnetic binary stars, Cuntz et al. [2000] and Saar et al. [2004] evaluated the reconnected power, again proportional to the magnetic energy density (thus to B^2) at the interaction point, and to the relative velocity between the interacting magnetic field lines. Even if the planet is weakly magnetized or unmagnetized, it will still drive an electrodynamic interaction with the star's magnetic field, similar in that case to the Io-Jupiter interaction. Through its induced magnetic field or UV-induced ionosphere, the planet will interact with the star's magnetic field by generating waves (Alfvén, slow mode...), in turn accelerating electrons along field lines towards the star's surface. The maximum dissipated power through this "unipolar" interaction can be again estimated according to expression (8) with $\varepsilon = 1$.

Following Zarka et al. [2001a], we can estimate the dissipated powers for exoplanets around a solar-type star (with a solar-type stellar wind) just based on the dependence of solar wind parameters (N, B, V) with the distance d to the Sun. To a first approximation, beyond a few R_S above the solar surface, V can be considered as constant, density N varies in $1/d^2$ (due to mass conservation during expansion), radial field B_r varies in $1/d^2$ (due to magnetic flux conservation), and azimuthal field along the Parker spiral $B_\phi = B_r \times \Omega d/V$ varies thus in $1/d$ (with $\Omega = 2\pi/P_S$ the solar rotation circular frequency; $P_S \sim 27$ days). For a better description close to the Sun, we have used the following expressions adapted from Hollweg [1999]:

$$\begin{aligned} B_r(G) &= 1.5/d^2 \times (1 + (f-1)/d^{1.5}) \\ B_\varphi &= B_r \times \Omega d/V \\ B_{tot} &= \sqrt{B_r^2 + B_\varphi^2} \end{aligned} \tag{10}$$

with $4 \leq f \leq 9$ the non-d^2 expansion factor (we use $f = 6.5$), and d expressed in units of solar radii;

$$N_e[\mathrm{cm}^{-3}] = 3 \times 10^8 d^{-15} + 4 \times 10^6 d^{-4.5} + 2.3 \times 10^5 d^{-2} \tag{11}$$

providing $N_e = 5[\mathrm{cm}^{-3}]$ at the Earth orbit ($d = 1$ AU $= 213.7\ R_S$). Figure 5 shows the corresponding profiles for B_{tot} and N_e. The profile of V, plotted on Figure 6, has been deduced from energy density plots by Shatten [1972]. Other descriptions of B, N and V can be found in the literature but our results below are little dependent on the detailed formulas used.

The term $B_\perp$ entering eq. (8) is the SW magnetic field perpendicular to the flow in the planet's frame. Similarly, V represents the SW flow velocity in the planet's frame. For orbital distances of 1 to several AU, the flow direction can be taken along the Sun-planet

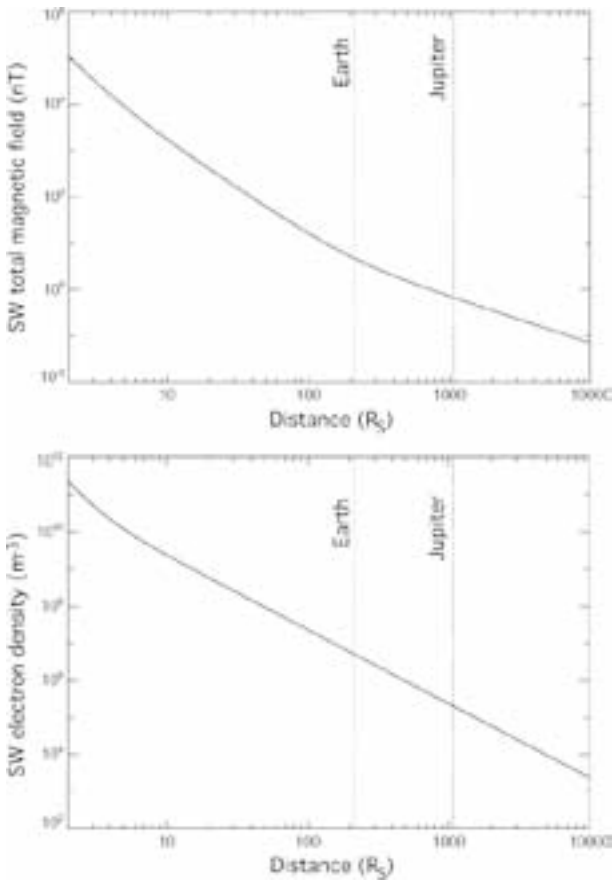

Figure 5: Typical profiles of the total SW magnetic field (B_{tot}, top) and electron density (N_e, bottom) versus distance to the Sun (see text). R_S is the solar radius (1 $R_S = 7 \times 10^8$ m). Orbits of the Earth (1 $AU = 213.7\ R_S$) and Jupiter are indicated.

line and the planetary orbital speed can be neglected relative to the flow speed (V_{SW} in the Sun's frame). This is no more true for hot Jupiters at $0.05 - -0.1$ AU orbital distance. Figure 6 displays the orbital velocity $V_{orb} = \sqrt{GM_S/d}$ versus the distance to the Sun, and the "effective" flow velocity in the planet's frame ($\mathbf{V} = \mathbf{V}_{SW} - \mathbf{V}_{orb}$). Due to the large orbital velocities close to the Sun, V remains everywhere above ~ 300 km/s instead of steeply decreasing below $\sim 10\ R_S$. $B_\perp$ is then calculated as:

$$B_\perp = B \times |\sin(\alpha - \beta)| \tag{12}$$

with

$$\alpha = \arctan(B_\varphi/B_r) \quad \text{and} \quad \beta = \arctan(V_{orb}/V_{SW})$$

Figure 7 (top) displays a sketch of the corresponding geometry, and Figure 7 (bottom)b shows plots of $\alpha(d)$ and $\beta(d)$. Figure 8 displays variations of $|\mathbf{B}|$, B_ϕ, B_r, and $B_\perp$ versus the distance. Far from the Sun $B_\perp$ varies as B_φ (i.e. in $1/d$) while close to the Sun, it varies as B_r (i.e. in $1/d^2$). In between, at $d \sim 37\ R_S$, $B_\perp$ goes through a deep minimum where the effective flow velocity is along the Parker spiral.

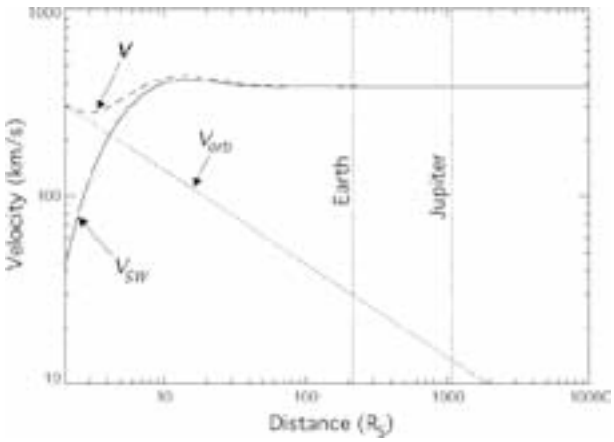

Figure 6: Typical SW velocity profile (see text). V_{SW} is the flow speed in the Sun's frame, V_{orb} the Keplerian orbital velocity versus distance, and **V** *the resulting SW flow velocity in the planet's frame. Note that the latter remains high even close to the Sun.*

It is then easy to compute and plot versus distance (on Figure 9) the dissipated magnetic power per unit area ($VB_{\perp}^2/\mu_o$). On the same figure is superimposed the dissipated kinetic (flow) power per unit area (NmV^3). We note that the magnetic power becomes comparable to the kinetic one at about 10 R_S distance, while their ratio is constant and ~ 170 beyond about 100 R_S(~ 0.5 AU). The kinetic power at the orbit of a hot Jupiter (0.05 AU) is found 2×10^4 times larger than at Jupiter's orbit (5.2 AU), and this ratio is 6×10^5 times for the magnetic power.

A strongly magnetized hot Jupiter will thus experience a much stronger magnetospheric interaction than Jupiter's one. But magnetospheric compression must also be taken into account. The magnetopause radius is fixed by the pressure equilibrium between the planetary magnetic field and the solar wind ram pressure:

$$R_{\mathrm{MP}} = R_P \times \left[2\frac{B_P^2}{K\mu_o NmV^2}\right]^{1/6} \tag{13}$$

with R_P the planetary radius, B_P the planet's equatorial surface field, $K = 1 - -2$ depending on details of SW particle reflection at the magnetopause, and N, m, V characterizing the SW. The much higher pressure at 0.05 AU results in a highly compressed magnetosphere (by a factor ~ 5), as illustrated on Figure 10 for a planetary magnetic field equal to Jupiter's. Finally, the dissipated (magnetic) power as defined by eq. (8) is $6 \times 10^5/5^2 = 2.4 \times 10^4$ times larger for a Jovian-like hot Jupiter at 0.05 AU than for Jupiter itself. This factor largely exceeds 10^5 for the closest hot-Jupiters (at 0.02–0.03 AU from their parent star). If kinetic input power to the magnetosphere is considered, the gain is only a factor $\sim 10^3$ relative to Jupiter (Figure 11).

Extrapolation of the Radio-Magnetic Bode's law of Figure 1 using the above dissipated powers imply that hot Jupiters may produce radio emissions 10^3 to 10^5 times more intense than Jupiter, if no unexpected "saturation" mechanism occurs which would prevent to reach such high radio fluxes. Note again that only the case of a Sun-like star and wind

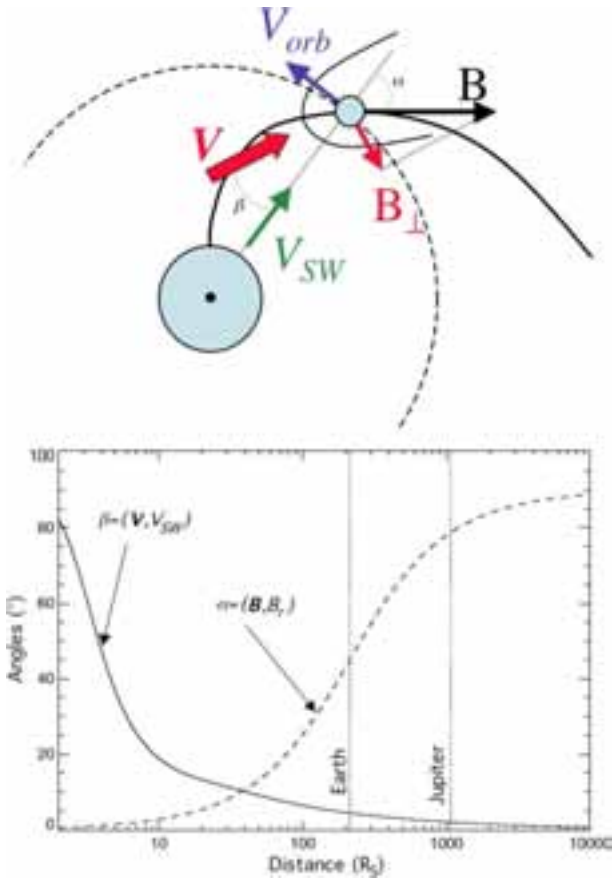

*Figure 7: Top: sketch of the geometry of the SW flow and magnetic field at a planetary orbit. The IMF (**B**) is tangent to the Parker spiral. $B_\perp$ is the SW field perpendicular to the flow in the planet's frame, which enters in the IMF Poynting flux onto the magnetospheric cross-section. Bottom: variation of the angles defined in the figure (and in section 4.1) versus distance to the Sun.* **V** *and* **B** *are aligned at $d \sim 37\ R_S$.*

has been considered here. Extension of the above analysis to a parametric study of the influence of V, B, ... remains to be done.

4.2 Unipolar / Dipolar interaction

In addition to the above SW-magnetosphere interaction leading to auroral planetary emissions, another type of planet-star interaction will occur independent of the fact that the planet is strongly, weakly or not magnetized. This interaction is the one described in section 2 for Jupiter-satellite interactions, with the star playing the role of Jupiter and the exoplanet that of the satellite. The similarity is further supported by the fact that the solar wind is sub-Alfvénic beyond distances about 15 R_S (~ 0.07 AU) from the Sun, in the frame of the description by equations (10–11). Sub-Alfvénic regime is indeed necessary for Alfvén waves to be able to propagate from the planet to the star. Figure 12 displays the Alfvén Mach number $M_A = V/V_A \approx V \times \sqrt{1.1 \times \mu_o N m_p}/B_{tot}$ as a function of the distance to the Sun. The sub-Alfvénic region expands for a stronger stellar field B

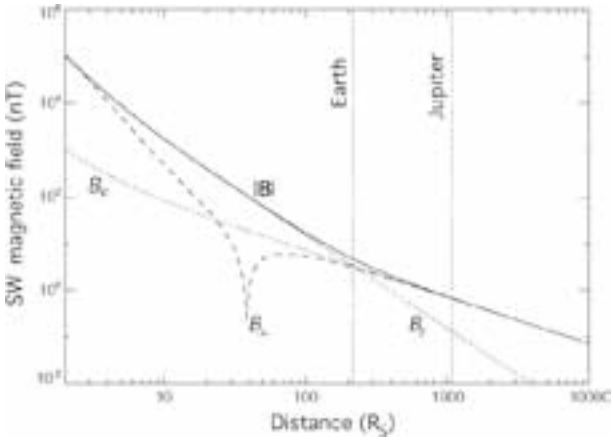

Figure 8: Variations with distance of total IMF magnitude $|\mathbf{B}|$*, azimuthal and radial components* $B\varphi$*,* B_r*, and perpendicular component* $B_\perp$*.*

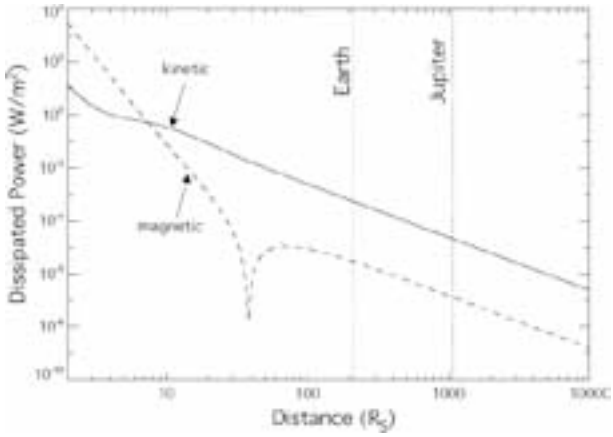

Figure 9: Dissipated SW magnetic power $(VB_\perp^2/\mu_o)$ *and kinetic* (NmV^3) *power per unit area. They become comparable at a distance about* 10 R_S*.*

and/or a lower wind density N. The system formed by a hot Jupiter and its magnetized parent star is thus a giant analogous to the Io-Jupiter or Ganymede-Jupiter systems. The dissipated power through reconnection or Alfvén (or slow mode) waves can thus be estimated according to eq. (8), and the radio power emitted by accelerated electrons along the star's magnetic field lines via eq. (9).

However, an important difference exists with respect to Jupiter. At Jupiter, the ionospheric plasma density decreases exponentially above a peak at $N_e \sim 3.5 \times 10^5$ cm^{-3} with a topside scale height of $\sim$ 1000 km [Hinson et al., 1998], while the dipolar magnetic field decreases in $1/R^3$ from a surface value of 4 to 14 G. Thus the ratio f_{pe}/f_{ce} between the plasma frequency ($f_{pe} = (1/2\pi)\sqrt{N_e e^2/\varepsilon_o m_e} \sim 9\sqrt{N_e}$ with f_{pe} in kHz and N_e in cm^{-3}) and the cyclotron frequency ($f_{ce} = eB/2\pi m_e = 2.8B$ with f_{ce} in MHz and B in G) is everywhere ≤ 0.14, the critical threshold value below which efficient wave amplification by the cyclotron-Maser instability is allowed [Le Quéau et al., 1985; Zarka, 1998; Zarka

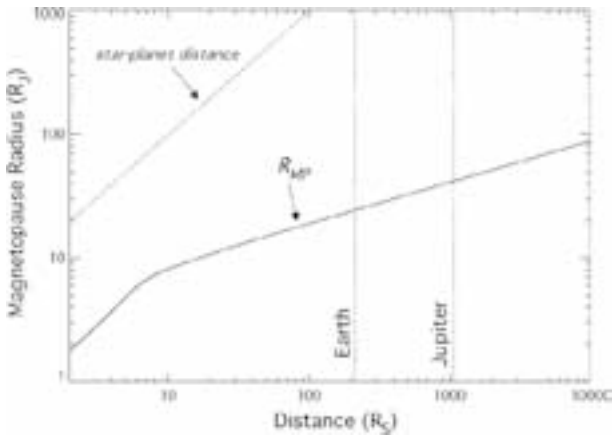

Figure 10: Radius of the magnetopause cross-section versus the distance to the Sun for a planet with magnetic dipole equal to Jupiter. At 10 R_S*, the magnetosphere is compressed by a factor* $\sim$ 5 *relative to Jupiter's magnetosphere at 5 AU. For a Jovian-like field, the magnetosphere of a hot Jupiter remains much smaller than the star-planet separation at all orbital distances.*

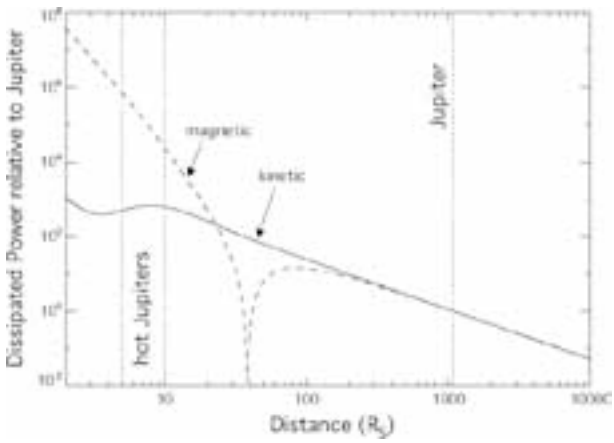

Figure 11: Dissipated SW magnetic and kinetic powers for a Jovian-like hot Jupiter, relative to the case of Jupiter itself. For hot Jupiters, the ratio for kinetic powers is $\sim 10^3$ *while it exceeds* 2×10^4 *for magnetic powers (up to several times* 10^5*).*

et al., 2001b]. By contrast, the solar corona has on the average $f_{pe}/f_{ce} \geq 1$, (Figure 13, κ=1) forbidding thus cyclotron-Maser emission at the fundamental of the X mode, by far the most efficient process of radio emission generation. Fundamental O mode or second harmonic O and X mode emissions remain possible, but with an efficiency at least 20 to 30 dB lower than fundamental X mode [Ashwanden and Benz, 1988; Treumann, 2000].

Fundamental X mode emission becomes possible for f_{ce} 10 to 100 times higher than in the solar case (Figure 13, κ=10–100), i.e. in strongly magnetized localized regions of the solar or stellar surface, or in the case of a strongly magnetized star. The two consequences are: (i) Radio emission is produced at higher frequency than in the case of magnetospheric interaction, where the expected cyclotron frequencies are or the order of that of Jupiter, i.e. tens of MHz; the cyclotron frequencies derived from eq. (10) for the Sun are between

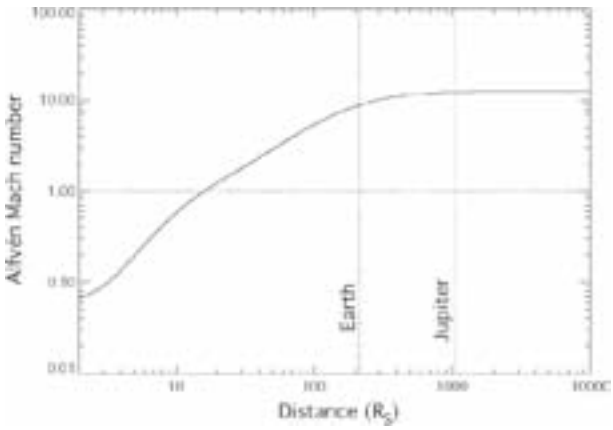

Figure 12: Alfvén Mach number versus distance to the Sun. The SW becomes sub-Alfvénic within about 15 R_S.

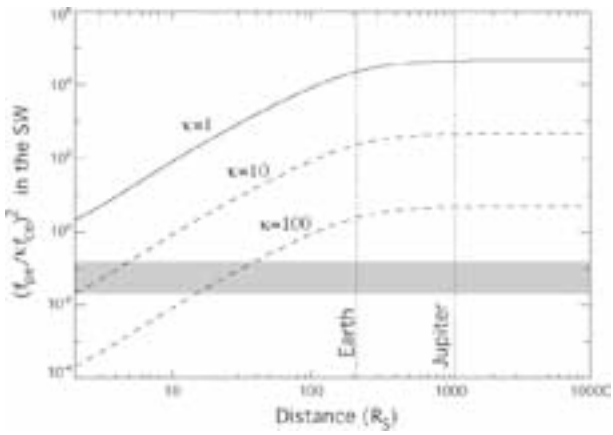

Figure 13: Ratio $(f_{pe}/(\kappa f_{ce}))^2$ *versus distance. The shaded region indicates the upper limit of this factor still compatible with radio wave generation/amplification via the cyclotron-maser mechanism. It requires stars* ≥ 100 *times as strongly magnetized as the Sun* ($\kappa = 100$) *to allow cyclotron-Maser operation at the orbit of hot Jupiters.*

3 MHz at 2 R_S and 25 MHz at 1 R_S (solar surface, out of spot regions); thus in the case of unipolar (or dipolar) interaction with a stellar magnetic field at least 10 times stronger than the Sun's, the radio frequencies emitted by the precipitating electrons in the 1–2 R_S altitude range above the stellar surface would be $\geq 30 - 250$ MHz. (ii) The dissipated power can again be estimated via eq. (8) and is thus that of the magnetospheric interaction multiplied by a factor $(R_{\text{exo-ionosphere}}/R_{\text{magnetosphere}})^2 \times (B_{\text{star}}/B_{\text{Sun}})^2$; the typical radius of the exo-ionosphere of a hot Jupiter is $\sim 2\ R_J$ [see e.g. Vidal-Madjar et al., 2003] versus $\sim 8\ R_J$ for the magnetosphere of a Jupiter at 0.05 AU (Figure 10), thus for $B_{\text{star}} = 10 \times B_{\text{Sun}}$, the above multiplying factor is $(2/8)^2 \times (10)^2 \sim 6$.

Unipolar interaction between a hot Jupiter and a magnetic star (or strongly magnetized regions of the stellar surface) is thus expected to produce radio emission up to 10^6 times that of Jupiter at frequencies of tens to hundreds of MHz, again if no unexpected "sat-

uration" mechanism prevents intense radio emission generation (Figure 1). The specific case of a system including a magnetic white dwarf and a second body that may be another white dwarf (possibly non-magnetic) or a planet has been studied by Willes and Wu [2004, 2005]. More generally, radio flares from magnetic stars, especially if they are periodic, could be driven by the presence of a close-in orbiting exoplanet playing the role of a unipolar inductor. This is precisely the reason invoked by Rubenstein and Schaefer [2000] and Schaefer et al. [2000] to explain the radio "superflares" that they have discovered originating from a few stars. The search for periodicities in the radio emission of known flaring stars could allow to test the presence of a planetary companion.

5 The case of HD179949

Shkolnik et al. [2003, 2004] have studied the spectrum of several stars, known from radial velocity measurements to possess a hot Jupiter, to search for periodic variation of chromospheric lines at the planetary orbital period. They found such variations (at $\sim 2.7\%$ level) in the Ca II H and K lines (393.3 and 396.8 nm) of the star HD179949, with a period consistent with the 3.093 day revolution period of the planet orbiting it at 0.045 AU, while the star's rotation period was estimated to be about 6–10 days [Saar et al., 2004]. They interpreted this periodic variation of the chromospheric activity as driven by magnetic reconnection between the magnetic fields of the two bodies, leading to charged particles precipitation towards the star's surface resulting in a chromospheric optical hot spot. This hot spot was tentatively found to lie $\sim 60°$ longitude ahead of the planet's orbital position. As the planet is likely to be tidally spin-orbit synchronized, its magnetic field may be weak, resulting in a unipolar inductor-like interaction. We comment here two aspects of HD 179949: the dissipated power and the longitudinal shift of the hot spot.

The maximum dissipated power can be estimated again from eq. (8) setting $\varepsilon = 1$. From Figure 9, we derive a magnetic power flux ~ 0.15 W/m^2, and a kinetic (flow) power flux 3 times as high, at an orbital distance of 0.045 AU or 9 R_S. The maximum dissipated power per Jovian radius of the obstacle is thus $\sim 0.15 \times \pi R_J^2 = 2 \times 10^{15}$ W. How does this number compare with the required power for a chromospheric spot increasing the star's brightness by 2.7% in the Ca II H and/or K lines? Solar optical brightness is $\sim 10^{13}$ Wm^{-1}m^{-2}sr^{-1}, so that the power P corresponding to 2.7% of the intensity of a 0.3 Ångström-wide line of intensity being $\sim 1/3$ of the stellar continuum [Shkolnik et al., 2003] is:

$$P \sim 10^{13} \times 0.3 \times 10^{-10} \times 2\pi^2 R_S^2 \times 0.027/3 \sim 3 \times 10^{19} \text{ W}$$

This estimate is consistent with that of Shkolnik et al. [2005]. In order for the dissipated power to match the emitted one, one needs a stellar magnetic field $\sim 30--100$ times that of the Sun (depending on the field topology), a wind strength larger than the Sun's, an obstacle size much larger than πR_J^2 due to a strong intrinsic planetary field or an extended exo-ionosphere, or a combination of these factors. From a slightly different approach, Shkolnik et al. [2005] reached similar conclusions about the star's magnetic field. Saar et al. [2004] noted that the wind strength is usually correlated with the stellar X-ray flux F_X, and Shkolnik et al. [2003] mentioned that in the case of HD179949, assumed to be

youngger than the Sun due to its short rotation rate, F_X is likely to be 10 times that of the Sun. As discussed in the previous section, existence of a radio emission associated with this possible magnetic planet-star interaction depends on the existence of a strong planetary or stellar magnetic field.

The 60° lead angle of the chromospheric hot spot relative to the sub-planet point raises another problem: the lead angle of the Io-induced UV/IR/Radio emissions relative to Io's instantaneous longitude is most of the time positive because Jupiter's rotation period is shorter than Io's orbital period so that the "downstream" direction in the Io-Jupiter interaction is ahead of Io's relative to its orbital motion. But in the case of HD179949, the planetary orbital period is much shorter than the estimated stellar rotation. If induced by the planet, the chromospheric hot spot should lag the instantaneous longitude of the planet (in the star's frame). The observed lead angle may be explained by a combination of the following effects :

- the Parker's spiral at 0.045 AU, which implies (with $V < 400$ km/s [Preusse et al., 2005]) a longitude shift $> +10°$ between the point of the stellar surface magnetically connected to the planet and the planet itself;
- a distorted stellar magnetic field geometry (non-meridian field lines) consistent with the fact that HD179949 is a rapid rotator (6–10 day period);
- a tilt between the star's rotation axis and magnetic dipole axis.

The latter two effects should lead to alternatively positive and negative longitude shifts, difficult to reconcile (even with a selection effect of the observations) with an apparently stable lead angle of 60°. Another possibility is that the 60° lead is actually a 300° lag due to propagation of the planet-driven Alfvén perturbation in the expanding stellar wind flow.

The observations of Shkolnik et al. [2003] thus raise questions in terms of both the dissipated power and the longitudinal shift of the chromospheric hot spot. This first detection of a planet-driven chromospheric activity (recently completed by a second detection - of ν And by [Shkolnik et al., 2005]) now requires further analyses.

6 Conclusions and Observations

Based on the observed correlation in our solar system between the output planetary radio power and the SW power incident on the magnetopause, and on the energetics of the interaction between Jovian moons and Jupiter's magnetic field (through Alfvén waves or magnetic reconnection), we have derived a "generalized Radio-Magnetic Bode's law" relating the output radio power of a magnetized flow-obstacle system to the magnetic energy flux convected on the obstacle (as defined by equations (8) and (9)). A similar scaling law may also apply to some extent to satellite-induced UV emissions within the Jovian system.

Extrapolation of the Radio-Magnetic Bode's law to the case of hot Jupiters suggests that these planets may produce very intense radio emissions due to either magnetospheric interaction with a strong stellar wind or unipolar interaction between the planet and a magnetic star (or strongly magnetized regions of the stellar surface). In the former case, similar to the magnetosphere-solar wind interactions in our solar system or to the Ganymede-Jupiter interaction, a hecto-decameter emission is expected in the vicinity of the planet with an intensity 10^3 to 10^5 times that of Jupiter's low frequency radio emissions. In the latter case, which is a giant analogous of the Io-Jupiter system, emission in the decameter-to-meter wavelength range near the footprints of the star's magnetic field lines interacting with the planet may reach 10^6 times that of Jupiter (unless some "saturation" mechanism occurs).

The system of HD179949 might be a good candidate for detection in the radio range, if the planet or the star is strongly magnetized. Discussion of the results of Shkolnik et al. [2003] (nearly sub-planetary optical chromospheric hot spot) at the light of eq. (8) nevertheless raise problems in terms of both the dissipated power and the longitude of the chromospheric hot spot, requiring thus confirmation of the detection.

As discussed by Zarka [2004], a radio emission 10^3 to 10^5 times as intense as Jupiter's decameter emission should be detectable at several tens of parsecs range with present (VLA, UTR-2, GMRT) or future (LOFAR) large ground-based instruments. Searches have been conducted with the VLA (New Mexico) at 74 and 330 MHz [Bastian et al., 2000; Farrell et al., 2003, 2004b], with UTR-2 (Kharkov, Ukraine) in the range 18–32 MHz [Zarka et al., 1997; Ryabov et al., 2004], and with the GMRT (India) at 150 MHz [Winterhalter et al., 2005]. The results are still negative, but upper limits of undetected emissions are steadily getting closer to predicted fluxes. The LOw Frequency ARray (LOFAR – `www.lofar.org`; Kassim et al. [2004]; Farrell et al. [2004a]), which should start operation in 2007, will offer an unprecedented sensitivity in the range 10–240 MHz. This sensitivity should allow detection of radio exoplanets if the extrapolations discussed above are valid.

Beyond direct detection of exoplanetary radio photons, low-frequency (decameter) radio observations of exoplanets are expected to provide estimates of their rotation period and their magnetic field (putting strong constraints on scaling laws and internal structure models), and invaluable inputs for extending comparative magnetospheric physics [Zarka et al., 1997; Farrell et al., 2004a].

References

Akasofu, S.-I., Energy coupling between the solar wind and the magnetosphere, *Space Sci. Rev.*, **28**, 121–190, 1981.

Akasofu, S.-I., Interaction between a magnetized plasma flow and a strongly magnetized celestial body with an ionized atmosphere, *Ann. Rev. Astron. Astrophys.*, **20**, 117–138, 1982.

Aschwanden, M. J., and A. O. Benz, On the electron cyclotron Maser instability, II, Pulsations in the quasi-stationary state, *Astrophys. J.*, **332**, 446–475, 1988.

Barrow, C. H., and M. D. Desch, Solar wind control of Jupiter's hectometric radio emission, *Astron. Astrophys.*, **213**, 495–501, 1989.

Bastian, T. S., G. A., Dulk, and Y. Leblanc, A Search for Radio Emission from Extrasolar Planets, *Astrophys. J.*, **545**, 1058–1063, 2000.

Burns, J. A., The evolution of satellite orbits, in Satellites, edited by J. A. Burns and M. S. Matthews, University of Arizona Press, pp. 117–158, 1986.

Clarke, J. T., J. Ajello, G. Ballester, L. B. Jaffel, J. Connerney, J.-C. Gérard, G. R. Gladstone, D. Grodent, W. Pryor, J. Trauger, and J. H. Waite, Ultraviolet auroral emissions from the magnetic footprints of Io, Ganymede, and Europa on Jupiter, *Nature*, **415**, 997–1000, 2002.

Connerney, J. E. P., Doing more with Jupiter's magnetic field, in Planetary Radio Emissions III, edited by H. O. Rucker, S. J. Bauer, and M. L. Kaiser, Austrian Acad. Sci. press, Vienna, pp. 13–33, 1992.

Connerney, J. E. P., M. H. Acuña, N. F. Ness, and T. Satoh, New models of Jupiter's magnetic field constrained by the Io flux tube footprint, *J. Geophys. Res.*, **103**, 11929–11939, 1998.

Connerney, J. E. P., R. Baron, T. Satoh, and T. Owen, Images of excited H3+ at the foot of the Io flux tube in Jupiter's atmosphere, *Science*, **262**, 1035–1038, 1993.

Cuntz, M., S. H. Saar, and Z. E. Musielak, On stellar activity enhancement due to interactions with extrasolar giant planets, *Astrophys. J.*, **533**, L151–L154, 2000.

Desch, M. D. and M. L. Kaiser, Saturn's kilometric radiation – Satellite modulation, *Nature*, **292**, 739–741, 1981.

Desch, M. D., and M. L. Kaiser, Predictions for Uranus from a radiometric Bode's law, *Nature*, **310**, 755–757, 1984.

Desch, M. D., and H. O. Rucker, The relationship between Saturn kilometric radiation and the Solar wind, *J. Geophys. Res.*, **88**, 8999–9006, 1983.

Erkaev, N. V., V. A. Shaidurov, V. S. Semenov, and H. K. Biernat, Effects of MHD slow shocks propagating along magnetic flux tubes in a dipole magnetic field, *Nonlinear Processes in Geophysics*,**9**, 163–172, 2002.

Farrell, W. M., M. D. Desch, and P. Zarka, On the possibility of coherent cyclotron emission from extrasolar planets, *J. Geophys. Res.*, **104**, 14025–14032, 1999.

Farrell, W. M., T. J. Lazio, M. D. Desch, T. Bastian, and P. Zarka, Limits on the Magnetosphere/Stellar Wind Interactions for the Extrasolar Planet about Tau Bootes, *ASP Conf. Ser.* **294**: Scientific Frontiers in Research on Extrasolar Planets, 151–156, 2003.

Farrell, W. M., T. J. Lazio, P. Zarka, T. Bastian, M. D. Desch, and B. P. Ryabov, The Radio Search for Extrasolar Planets with LOFAR, *Planet. Space Sci.*, **52**, 1469–1478, 2004a..

Farrell, W. M., T. J. W. Lazio, M. D. Desch, T. S. Bastian, and P. Zarka, Radio Emission from Extrasolar Planets, Bioastronomy 2002: Life Among the Stars, Proceedings of IAU Symposium #213. Edited by R. Norris, and F. Stootman. San Francisco: Astronomical Society of the Pacific, 2003., 73, 2004b.

Goldreich, P., and D. Lynden-Bell, Io: A Jovian unipolar inductor, *Astrophys. J.*, **156**, 59–78, 1969.

Griessmeier, J.-M., U. Motschmann, G., Mann, and H. O. Rucker, The influence of stellar wind conditions on the detectability of planetary radio emissions, *Astron. Astrophys.*, **437**, 717–726, 2005.

Griessmeier, J.-M., A. Stadelmann, T. Penz, H. Lammer, F. Selsis, I. Ribas, E. F. Guinan, U. Motschmann, H. K. Biernat, and W. W. Weiss, The effect of tidal locking on the magnetospheric and atmospheric evolution of "hot Jupiters", *Astron. Astrophys.*, **425**, 753–762, 2004..

Gurnett, D. A., W. S. Kurth, A. Roux, S. J. Bolton, and C. F. Kennel, Evidence for a magnetosphere at Ganymede from plasma wave observations by the Galileo spacecraft, *Nature*, **384**, 535–537, 1996.

Gurnett, D. A., A. M. Persoon, W. S. Kurth, A. Roux, S. J Bolton, and C. F. Kennel, Plasma densities in the vicinity of Callisto from Galileo plasma wave observations, *Geophys. Res. Lett.*, **27**, 1867–1870, 2000.

Hinson, D. P., J. D. Twicken, and E. T. Karayel, Jupiter's ionosphere: new results from Voyager 2 radio occultation measurements, *J. Geophys. Res.*, **103**, 9505–9520, 1998.

Hollweg, J. V., Potential wells, the cyclotron resonance, and ion heating in coronal holes, *J. Geophys. Res.*, **104**, 505–520, 1999.

Hospodarsky, G. B., I. W. Christopher, J. D. Menietti, W. S. Kurth, D. A. Gurnett, T. F. Averkamp, J. B. Groene, P. Zarka, Control of Jovian radio emissions by the galilean moons as observed by Cassini and Galileo, in Planetary Radio Emissions V, edited by H. O. Rucker, M. L. Kaiser and Y. Leblanc, Austrian Acad. Sci. Press, Vienna, pp. 155–164, 2001.

Kaiser, M. L., P. Zarka, W. S. Kurth, G. B. Hospodarsky, and D. A. Gurnett, Cassini and Wind stereoscopic observations of Jovian non-thermal radio emissions : measurements of beamwidths, *J. Geophys. Res.*, **105**, 16053–16062, 2000.

Kassim, N. E., T. J. W. Lazio, P. S. Ray, P. C. Crane, B. C. Hicks, K. P. Stewart, A. S. Cohen, and W. M. Lane, The low-frequency array (LOFAR): opening a new window on the universe, *Planet. Space Sci.*, **52**, 1343–1349, 2004.

Khurana, K. K., M. G. Kivelson, D. J. Stevenson, G. Schubert, C. T. Russell, R. J. Walker, and C. Polanskey, Induced magnetic fields as evidence for subsurface oceans in Europa and Callisto, *Nature*, **395**, 777–780, 1998.

Kivelson, M. G., K. K. Khurana, C. T. Russell, R. J. Walker, J. Warnecke, F. V. Coroniti, C. Polanskey, D. J. Southwood, and G. Schubert, Discovery of Ganymede's magnetic field by the Galileo spacecraft, *Nature*, **384**, 537–541, 1996.

Kivelson, M. G., K. K. Khurana, F. V. Coroniti, S. Joy, C. T. Russell, R. J. Walker, J. Warnecke, L. Bennett, and C. Polanskey, The magnetic field and magnetosphere of Ganymede, *Geophys. Res. Lett.*, **24**, 2155–2158, 1997a.

Kivelson, M. G., K. K. Khurana, C. T. Russell, R. J. Walker, P. J. Coleman, F. V. Coroniti, J. Green, S. Joy, R. L. McPherron, C. Polanskey, D. J. Southwood, L. Bennett, J. Warnecke, and D. E. Huddleston, Galileo at Jupiter — Changing states of the magnetosphere and first looks at Io and Ganymede, *Adv. Space Res.*, **20**, 193–204, 1997b.

Kivelson, M. G., F. Bagenal, W. S. Kurth, F. M. Neubauer, C. Paranicas, and J. Saur, Magnetospheric interactions with satellites, in Jupiter : The Planet, Satellites, and Magnetosphere, edited by F. Bagenal, W. McKinnon and T. Dowling, Cambridge University Press, Chapter 21, pp. 513–536, 2004.

Knight, S., Parallel electric fields, *Planet. Space Sci.*, **21**, 741–750, 1973.

Kurth,W.S., D.A. Gurnett, and F.L. Scarf, Control of Saturn's kilometric radiation by Dione, *Nature*, **292**, 742–745, 1981.

Kurth, W. S., D. A. Gurnett, and J. D. Menietti, The influence of the Galilean satellites on radio emissions from the Jovian system, in Radio Astronomy at Long Wavelengths, edited by R. G. Stone, K. W. Weiler, M. L. Goldstein, and J.-L. Bougeret, *Geophysical Monograph* **119**, AGU, Washington, DC, 213–225, 2000.

Le Quéau, D., R. Pellat, and A. Roux, The Maser synchrotron instability in an inhomogeneous medium: Application to the generation of auroral kilometric radiation, *Ann. Geophys.*, **3**, 273–292, 1985.

Menietti, J. D., D. A. Gurnett, W. S. Kurth, and J. B. Groene, Control of Jovian radio emission by Ganymede, *Geophys. Res. Lett.*, **25**, 4281–4284, 1998..

Menietti, J. D., D. A. Gurnett, and I. Christopher, Control of Jovian radio emission by Callisto, *Geophys. Res. Lett.*, **28**, 3047–3050, 2001.

Neubauer, F. M., Nonlinear standing Alfvén wave current system at Io: Theory, *J. Geophys. Res.*, **85**, 1171–1178, 1980.

Prangé, R., D. Rego, D. Southwood, P. Zarka, S. Miller, and W. Ip, Rapid energy dissipation and variability of the Io-Jupiter electrodynamic circuit, *Nature*, **379**, 323–325, 1996.

Prangé, R., D. Rego, L. Pallier, J. E. P. Connerney, P. Zarka, and J. Queinnec, Detailed study of FUV Jovian auroral features with the post-COSTAR Hubble Faint Object Camera, *J. Geophys. Res.*, **103**, 20195–20215, 1998.

Prangé, R., and P. Zarka, Planetary Aurorae, Invited paper #GAIII.14/07P/A12-007 (Abstract book p. B-242) at 23th IUGG General Assembly, Sapporo, Japan, 29/6-11/7/2003

Preusse, S., A. Kopp, J. Büchner, and U. Motschmann, Stellar wind regimes of close-in extrasolar planets, *Astron. Astrophys.*, **434**, 1191–1200, 2005..

Priest, E. R., The Sun and its magnetohydrodynamics, in Introduction to Space Physics, edited by M. G. Kivelson and C. T. Russell, *Cambridge University Press*, 58–90, 1995.

Queinnec, J., and P. Zarka, Flux, power, energy and polarization of Jovian S-bursts, *Planet. Space Sci.*, **49**, 365–376, 2001..

Rubenstein, E. P., and B. E. Schaefer, Are superflares on solar analogues caused by extrasolar planets?, *Astrophys. J.*, **529**, 1031–1033, 2000.

Ryabov, V. B., P. Zarka, and B. P. Ryabov, Search of exoplanetary radio signals in the presence of strong interference : Enhancing sensitivity by data accumulation, *Planet. Space Sci.*, **52**, 1479–1491, 2004.

Saar, S. H., Recent Measurements of Stellar Magnetic Fields, in Stellar surface structure, IAU Symp. 176, edited by K. G. Strassmeier and J. L. Linsky, Kluwer Academic Pub., Dordrecht, p. 237, 1996.

Saar, S. H., M. Cuntz, and E. Shkolnik, Stellar Activity Enhancement by Planets: Theory and Observations, in Stars as suns : activity, evolution and planets, IAU Symp. 219, edited by A. K. Dupree and A. O. Benz, Astronomical Society of the Pacific (ASP), San-Francisco, p. 355, 2004.

Sanchez-Lavega, A., The magnetic field in giant extrasolar planets, *Astrophys. J.*, **609**, L87–L90, 2004.

Saur, J., F. M. Neubauer, J. E. P. Connerney, P. Zarka, and M. G. Kivelson, Plasma interaction of Io with its plasma torus, in Jupiter : The Planet, Satellites, and Magnetosphere, edited by F. Bagenal, W. McKinnon and T. Dowling, Cambridge University Press, Chapter 22, pp. 537–560, 2004.

Schaefer, B. E., J. R. King, and C. P. Deliyannis, Superflares on ordinary solar-type stars, *Astrophys. J.*, **529**, 1026–1030, 2000.

Schneider, J., `http://vo.obspm.fr/exoplanetes/encyclo/index.php`, 2005.

Shatten, K. H., Solar activity observations and predictions, McIntosh and Dryer Eds., MIT Press, Cambridge, 1972.

Shkolnik, E., G. A. H. Walker, and D. A. Bohlender, Evidence for planet-induced chromospheric activity on HD 179949, *Astrophys. J.*, **597**, 1092–1096, 2003.

Shkolnik, E., G. A. H. Walker, and D. A. Bohlender, Erratim "Evidence for planet-induced chromospheric activity on HD 179949", *Astrophys. J.*, **609**, 1197, 2004.

Shkolnik, E., G. A. H. Walker, D. A. Bohlender, P.-G. Gu, and M. Kurster, Hot Jupiters and hot spots: the short- and long-term chromospheric activity on stars with giant planets, *Astrophys. J.*, **622**, 1075–1090, 2005.

Stevens, I. R., Magnetospheric radio emission from extrasolar giant planets : the role of the host stars, *Mon. Not. R. Astron. Soc.*, **356**, 1053–1063, 2005.

Treumann, R.A. Planetary radio emission mechanisms: a tutorial, in Radio Astronomy at Long Wavelengths, edited by R. G. Stone, K. W. Weiler, M. L. Goldstein, and J.-L. Bougeret, *Geophysical Monograph* **119**, AGU, Washington, DC, pp. 13–26, 2000.

Vidal-Madjar, A., Lecavelier des Etangs, A., Désert, J.-M., G. E. Balester, R. Ferlet, G. Hébrard, and M. Mayor, An extended upper atmosphere around the extrasolar planet HD209458b, *Nature*, **422**, 143–146, 2003.

Willes, A. J., and K. Wu, Electron-cyclotron maser emission from white dwarf pairs and white dwarf planetary systems, *Mon. Not. R. Astron. Soc.*, **348**, 285–296, 2004.

Willes, A. J., and K. Wu, Radio emissions from terrestrial planets around white dwarfs, *Astron. Astrophys.*, **432**, 1091–1100, 2005.

Winterhalter, D., G. Bryden, I. Chandra, W. Gonzalez, T. B. H. Kuiper, T. J. Lazio, W. Majid, R. A. Treumann, and P. Zarka, Search for radio emissions from extrasolar planets: the observation campaign, in *Planetary Radio Emissions VI*, H. O. Rucker, W. S. Kurth, and G. Mann (eds.), Austrian Academy of Sciences Press, Vienna, 2006, *this issue*.

Zarka, P., The auroral radio emissions from planetary magnetospheres: What do we know, what don't we know, what do we learn from them?, *Adv. Space Res.*, **12**, (8)99–(8)115, 1992.

Zarka, P., Auroral radio emissions at the outer planets: observations and theories, *J. Geophys. Res.*, **103**, 20159–20194, 1998.

Zarka, P., Nonthermal radio emissions from extrasolar planets, Extrasolar Planets: Today and Tomorrow, *Astronomical Society of the Pacific (ASP)*, Vol. **321**, edited by J.-P. Beaulieu, A. Lecavelier des Etangs and C. Terquem, San-Francisco, pp.160–169, 2004.

Zarka, P., Fast radio imaging of Jupiter's magnetosphere at low frequencies with LOFAR, *Planet. Space Sci.*, **52**, 1455–1467, 2004.

Zarka, P., T. Farges, B. P. Ryabov, M. Abada-Simon, and L. Denis, A scenario for jovian S-bursts, *Geophys. Res. Lett.*, **23**, 125–128, 1996.

Zarka, P., and F. Genova, Low frequency jovian emission and solar wind magnetic sector structure, *Nature*, **306**, 767–768, 1983.

Zarka, P., J. Queinnec, B. P. Ryabov, V. B. Ryabov, V. A. Shevchenko, A. V. Arkhipov, H. O. Rucker, L. Denis, A. Gerbault, P. Dierich, and C. Rosolen, Ground-Based High Sensitivity Radio Astronomy at Decameter Wavelengths, in Planetary Radio Emissions IV, edited by H. O. Rucker, S. J. Bauer, and A. Lecacheux, Austrian Acad. Sci. Press, Vienna, 101–127, 1997.

Zarka, P., R. A. Treumann, B. P. Ryabov, and V. B. Ryabov, Magnetically-driven planetary radio emissions and applications to extrasolar planets, *Astrophys. Space Sci*, **277**, 293–300, 2001a.

Zarka, P., J. Queinnec, and F. Crary, Low-frequency limit of Jovian radio emissions and implications on source locations and Io plasma wake, *Planet. Space Sci.*, **49**, 1137–1149, 2001b.

Zarka, P., B. Cecconi, and W. S. Kurth, Jupiter's low frequency radio spectrum from Cassini/RPWS absolute flux density measurements, *J. Geophys. Res.*, **109**, A09S15, doi:10.1029/2003JA010260, 2004.